Journal of Manufacturing Processes 169 (2026) 365–378

Contents lists available at ScienceDirect

Journal of Manufacturing Processes

journal homepage: www.elsevier.com/locate/manpro

Full length article

Predictive tool path compensation using ANN to minimize slenderness-induced errors in dry turning of UNS A97075-T6

S. Martín-Béjar [a,*], F.J. Trujillo [a], F. Bañón [a], C. Bermudo [a], L. Sevilla [a]

[a] Department of Civil, Materials and Manufacturing Engineering, University of Malaga, Malaga, Spain

ARTICLE INFO

Keywords:
Tool path
Artificial Neural Network
Dry turning
Geometrical error
Aluminium alloy

ABSTRACT

This study investigates dimensional deviations in dry turning of UNS A97075-T6 aluminium alloy, focusing on the impact of part slenderness and machining parameters. Experimental tests were conducted on specimens with varying diameters (10–18 mm), cutting speeds (40–80 m/min), and feed rates (0.05–0.15 mm/rev). Results reveal nonlinear deviation patterns, with maximum deviations up to 0.40 mm in slender parts. An iterative tool path compensation process reduced average deviations by 87%, achieving final errors below 0.10 mm. Based on these experiments, a feedforward Artificial Neural Network (ANN) was trained using diameter, cutting speed, and feed rate as inputs, and the compensated tool path as output. The ANN showed excellent predictive performance (R^2 = 0.98, RMSE = 0.0012 mm), enabling first-pass trajectory corrections without iteration. This approach improves part accuracy while reducing cost and time. The novelty lies in considering part slenderness as a key factor affecting final part dimensions to meet tolerance requirements. Additionally, the use of Artificial Neural Networks enables the inclusion of slenderness effects in tool path prediction, allowing for the correction of potential geometrical deviations. These results offer practical insights for enhancing dimensional control in manufacturing processes.

1. Introduction

The industry is subject to high demands in its production process in order to obtain parts that meet the design requirements. Among them, geometric tolerances (macrogeometric and microgeometric) and mechanical properties of the material are highly demanded [1,2]. Dimensional tolerances play an important role in components manufacturing, especially in production sectors that generate high-performance parts, such as the aeronautical, automotive or medical industries, among others. These tolerances are very narrow and demanding when manufactured parts intended to fit together [3,4].

The selection of the manufacturing process has a significant impact on the dimensions of the parts obtained. Casting [5], additive manufacturing [6,7] and hot plastic deformation processes [5] usually present a greater difficulty controlling these dimensional tolerances, mainly due to the thermal effect of the process. On the contrary, machining or cold plastic deformation processes generate smaller dimensional deviations of the manufactured part because this thermal effect is less significant [8].

Within machining operations, the development of automation allowed the generation of numerical control machining systems, which, by reducing human intervention in the process, reduced the geometric deviations of the manufactured parts. Therefore, considering the high demands of the aeronautical industry in terms of geometry control of aircraft components, machining operations using computer numerical control (CNC) machine tools are commonly used.

On the other hand, aluminium alloys are commonly used in aircraft manufacturing mainly because of their good relationship between density and mechanical properties [9]. Among these alloys, the aluminium zinc alloy UNS A97075 presents good machinability, making it a suitable material for aircraft structural elements or landing gear components [10].

Scientific community have reviewed key factors affecting aluminium alloy machinability, such as tool wear, surface roughness and power consumption under various machining conditions. In particular, Soren et al. [11] highlight the influence of feed rate, cutting speed and tool type on performance in dry and MQL environments. Santos et al. [12] provide a comprehensive review covering the influence of alloy composition, mechanical properties, thermal effects and tool wear on machining performance, highlighting the complexity of achieving

* Corresponding author.
E-mail address: smartinb@uma.es (S. Martín-Béjar).

https://doi.org/10.1016/j.jmapro.2026.04.074
Received 22 August 2025; Received in revised form 26 February 2026; Accepted 27 April 2026
Available online 2 May 2026

dimensional accuracy, especially under dry cutting conditions. Pimenov et al. [13] summarized the main strategies to improve machinability and surface integrity during the machining of aluminium alloys, including MQL, cryogenic cooling, vibration-assisted machining, tool coatings, and hybrid methods. Their analysis provides quantitative data on the influence of these strategies on roughness, tool wear, chip morphology, and energy consumption, offering a broad overview of the technological efforts made to enhance performance, particularly in dry conditions.

Despite the good machinability and process automation, machined parts often present deviations from their nominal geometry and may not meet design tolerances [14]. These errors are inherent to the machining process and are generally grouped into four categories: thermal effects [15], cutting forces [16], geometric/kinematic [17,18], and fixtures [19]. Thermal effects result from temperature increases in the cutting zone, causing material expansion and contraction, as well as affecting machine components. Cutting forces induce elastic deformations on the workpiece during material removal. Geometric and fixture-related errors arise from poor component selection, misalignment, or machine wear, which worsens over time despite maintenance efforts [20,21]. While some sources of error can be minimized with proper setup, others, such as those linked to cutting forces, vibrations, or temperature, cannot be entirely avoided. Therefore, reducing their impact through strategies like optimizing cutting parameters, tool configuration, or the use of cutting fluids becomes essential. Since cutting parameters such as cutting speed, feed rate, and depth of cut directly influence these effects, a strong relationship exists between their selection and the dimensional accuracy of the machined part.

D. Das et al. [22] analysed the influence of machining parameters on cutting temperature during dry turning of Al 7075-T6 using ZrCN-coated WC inserts. Their study found that minimum cutting temperatures occurred at the lowest spindle speed, feed rate, and depth of cut, with depth of cut being the most influential factor. Similar trends were reported in [23], where increased cutting speed and feed rate led to higher chip surface temperatures across various materials, including aluminium, titanium, and steel.

Concerning cutting forces, A. Srivastava et al. [24] reported that feed and depth of cut significantly increase cutting force values in dry turning of UNS A97075-T631, with depth of cut being the dominant factor. Cutting speed showed a less pronounced influence. Similar results were observed in different materials such as aluminium alloy UNS A96026-T9 [25], steel AISI D3 [26] or titanium alloy Ti6Al4V [27], with the depth of cut being the main cutting parameter that affects cutting forces.

Vibrations during turning operations are also influenced by cutting parameters. Loketcha et al. [28] experimentally analysed mild steel and found that cutting speed significantly affects vibrations in axial, tangential, and radial directions, while depth of cut only impacts axial vibrations, and feed rate has minimal influence. These findings are supported by results in [29], where dry turning of hardened steel revealed that increased spindle speed leads to higher tool vibrations, negatively impacting dimensional accuracy. Additionally, at high speeds, thermal effects become more pronounced, further compromising part geometry under dry conditions.

Regarding aluminium alloys, A. Şahinoğlu et al. [30] investigated the influence of cutting parameters on spindle vibration during turning of UNS A97075. Their findings indicated that feed rate had the strongest impact on vibration amplitude, while cutting speed and depth of cut had minimal influence. Based on the literature reviewed, cutting parameters directly influence dimensional deviations by affecting temperature, cutting forces, and vibrations. While such deviations cannot be entirely avoided, dimensional accuracy can be improved through appropriate selection of cutting conditions. However, this often involves using low parameter values, which increases machining time and may negatively affect properties like surface microhardness [31].

As an alternative, part accuracy in CNC machining can be improved by compensating deviations at the tool path level. For instance, M. Vaheby et al. [32] developed a software-based method to modify CNC tool paths based on estimated geometric and kinematic errors, achieving error reductions of up to 50% under mild milling conditions. Similarly, H. J. Pahk et al. [33] implemented a real-time thermal error compensation system using various predictive models. Their system corrected spindle and feed axis thermal deviations directly within the CNC controller, leading to an overall accuracy improvement of approximately 4–5 times.

Cutting tool wear is another significant source of dimensional deviations, as it alters the tool geometry during machining [34–36]. In [37], tool wear was analysed in turning of SAE 1018 steel by correlating it with vibration signals recorded throughout multiple operations. The study demonstrated that tool wear could be effectively monitored via vibration analysis, enabling real-time compensation during the machining process. The proposed approach achieved up to 93% correction in dimensional error, highlighting the potential of online wear detection for improving part accuracy.

The experimental approaches discussed previously often rely on a limited number of cutting parameter combinations, making it difficult to predict outcomes under untested conditions. Due to the high cost and time associated with extensive testing, predictive models such as Artificial Neural Networks (ANNs) have emerged as effective tools to relate input variables to machining outcomes.

ANNs have been widely applied in machining research. In [38], they were used to model and optimise drilling operations, linking cutting parameters to outputs such as roughness and thrust force. Similarly, ANNs have shown high accuracy in predicting machining time for standard parts, facilitating production planning [39]. In [40], an ANN successfully predicted surface roughness in milling of UNS A97075 using a small dataset, achieving a mean relative error below 1.25%. More advanced strategies, such as evolutionary neural networks [41], have been applied to automated toolpath planning, showing the importance of geometric inputs. Furthermore, deep neural networks have also been used for feature recognition in 3D CAD-integrated machining environments [42], highlighting the broad applicability of ANNs in improving machining performance and decision-making.

After a literature evaluation, it can be confirmed that there is a direct relationship between the cutting parameters and the dimensional deviations that can be generated in a machining operation. These parameters are variables of influence on the cutting temperature, cutting forces, or vibrations, which are the main causes of the errors generated in the geometry of the part. Although some studies consider that aim to analyse the influence of these causes on dimensional deviations, these should not be done individually as they are all part of the process. Furthermore, the slenderness of a part in a machining operation has not been considered and it is important due to the displacements that the cutting forces originate in the part during the machining process, which negatively affects the precision of the process.

Previous studies using neural networks in machining optimisation have mainly focused on cutting parameters, tool geometry, or measurable outputs such as surface roughness or tool wear. The geometrical configuration of the workpiece, particularly its slenderness, has not been explicitly included as an input variable because most available datasets correspond to short and rigid specimens where deformation effects are negligible and because slenderness has traditionally been analysed through analytical or finite element models rather than experimental data. This research addresses that limitation by incorporating slenderness as an ANN input variable, enabling the prediction of compensated tool paths that account for deformation effects in slender components.

Although numerous studies have explored the effects of machining parameters on surface finish, tool wear and cutting forces in aluminium alloys, the influence of part slenderness on dimensional deviation remains largely unexplored. This factor becomes especially critical in dry turning operations, where the absence of cutting fluids increases thermal and mechanical instability, making dimensional control more difficult. At the same time, industries such as aerospace and automotive increasingly rely on slender aluminium components that require high

Table 1
Tested alloy composition (% mass).

Zn	Mg	Cu	Cr	Si	Mn	Al
6.01	2.61	1.88	0.19	0.08	0.07	Rest

Table 2
Cutting parameters and final diameter.

v_c (m/min)	f (mm/rev)	a_p (mm)	D_n (mm)
40	0.05	1	18
80	0.15		16
			14
			12
			10

Table 3
Cutting angle setup.

Cutting angles	Value
Relief angle (α)	7°
Cutting edge angle (β)	66°
Rake angle (γ)	17°
Major cutting edge angle (κ_r)	62.5°
Insert include angle (ε)	55°
Tool nose radius (r_ε)	0.8 mm

accuracy without post-processing.

The novelty of this study lies in incorporating part slenderness, along with cutting parameters, into an ANN to directly predict a compensated tool path. This predictive approach aims to reduce deviations without iterative corrections, contributing to more efficient and sustainable manufacturing. To this end, different cutting speeds, feed rates and part diameters are tested experimentally to analyse the influence of slenderness on dimensional deviations. Therefore, the objective of this work is to evaluate the effect of part slenderness on the dimensional accuracy of dry turned components and to develop a predictive ANN capable of generating compensated tool paths that minimize geometrical deviations and bring the final part dimensions closer to the nominal values.

2. Materials and methodology

Several dry turning operations have been performed on the aeronautical aluminium alloy UNS A97075-T6. The removal of cutting fluids during machining was performed due to environmental reasons [43,44]. The composition (% mass) of the aluminium alloy was determined by arc atomic emission spectroscopy. The results are shown in Table 1. In addition, this allow presents a microhardness of 165 HV [45].

The initial stock corresponds to 20 mm diameter aluminium bars. A straight turning operation in a CNC turning centre was carried out with a machining length (L) of 230 mm, reducing the diameter to different values (D_n) to analyse the effect of the part slenderness on the dimensional deviations. In addition, cutting speed (v_c) and feed (f) values were varied during the cutting process, remaining constant the depth of cut (Table 2).

It should be noted that the cutting speed values suggested for the study are low for machining aluminium alloys. However, in the aeronautical industry, aluminium is sometimes combined with other materials to create fibre metal laminates (FML), such as CFRP + Al + Ti. In such cases, high cutting temperatures associated with high cutting speeds can cause damage to the material, which may result in delamination and deformation, requiring a reduction in the cutting speed value [46,47]. In addition, the selected feed values reflect typical values used in dry turning of aluminium alloys, particularly in aerospace applications where it is important to balance material removal efficiency with dimensional accuracy and are critical factors in the dimensional deviation of slender parts. The depth of cut remained constant at 1 mm in all cases to maintain consistency in the material removal process.

An uncoated WC–Co rhombic tool (ISO DCMT 11T308-14 IC20) was used in the turning operation. A new cutting edge has been used for each operation to avoid the effect of tool wear, ensuring that all operations are performed under the same conditions. The tool has been placed in a neutral position, with a main cutting-edge angle of 62.5°. This position is common in turning parts that have to generate sharp reductions in the machining diameter, avoiding a possible heeling of the tool with the workpiece, as well as allowing the possibility of machining in different directions without having to change the tool. The cutting angle setup is shown in Table 3.

After machining the specimens, the diameter was measured using a Mitutoyo QuantuMike digital micrometre (model 293-140-30), with a resolution of 0.001 mm, in different positions. The diameter was measured on 23 different circular sections 10 mm apart (Fig. 1), being the first position, the section resting on the tailstock of the lathe (Z_1–Z_{23}). In each section, 4 diameter measurements have been taken, considering the average value of the measurements obtained. Before taking the measurements, the instrument was calibrated, obtaining an overall uncertainty of 1 μm and a systematic correction of 1 μm, taking these values into account in the measurement of the diameters.

As the variation between repeated diameter measurements at each section was consistently below 0.005 mm, no further statistical analysis has been required. The results are presented using average values, as dispersion was negligible and did not affect the interpretation of the dimensional deviations.

A total of twenty turning tests were conducted combining different diameters, feed rates and cutting speeds, plus five additional validation trials. The variation between repeated measurements was below 0.005 mm, confirming the consistency of the dataset and its suitability for ANN training, in line with recent recommendations on data reliability for machine learning applications [48].

The acquired diametric measurements (D_{1i}) and their associated positions (Z_i) have been leveraged to adjust the cutting tool trajectory in a subsequent machining operation, with the objective of minimising dimensional deviations in the resultant part. At each specific position of the measured diameters (Z_i), a recalibrated tool position (X_i), adjusted from the nominal diameter, has been systematically accounted for. The adjusted position (X_i) has been obtained from the difference of D_{1i} (Eqs. (1) and (2)), providing a quantifiable means for this compensation.

$$\Delta D_{1i} = D_{1i} - D_n \tag{1}$$

$$X_{1i} = D_n - \Delta D_{1i} \tag{2}$$

This set of values assumes a new cutting tool path, which is used in the machining of new specimen. Once again, the diameter of the machined specimen (D_{2i}) is measured in each of the positions considered, and the deviation (ΔD_{2i}) with D_n has been considered. These results have been used to enact a further adjustment in the tool path (Eq. (4)).

$$\Delta D_{2i} = D_{2i} - D_n \tag{3}$$

$$X_{2i} = D_n - \Delta D_{1i} - \Delta D_{2i} \tag{4}$$

Finally, the turning process, followed by the measurement of the resulting part, was repeated, obtaining a new variation of the machined part with respect to the nominal value. This resulted in a new correction of the cutting tool path (ΔD_{3i}) as defined in Eq. (5). This last compensation was implemented (Eq. (6)) to guarantee that the machined part has a dimensional error less than 0.1 mm concerning the nominal value.

$$\Delta D_{3i} = D_{3i} - D_n \tag{5}$$

$$X_{3i} = D_n - \Delta D_{1i} - \Delta D_{2i} - \Delta D_{3i} \tag{6}$$

A feedforward neural network has been developed to predict the

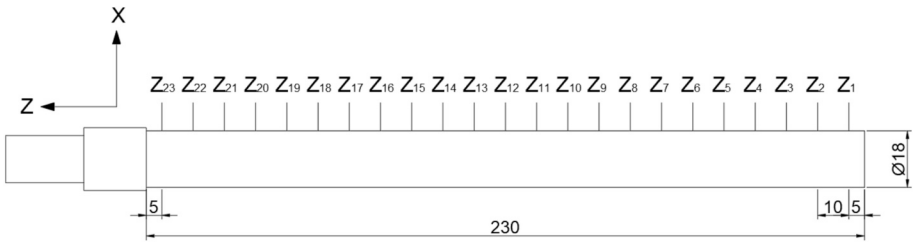

Fig. 1. Sections measured after turning operations (dimensions in mm).

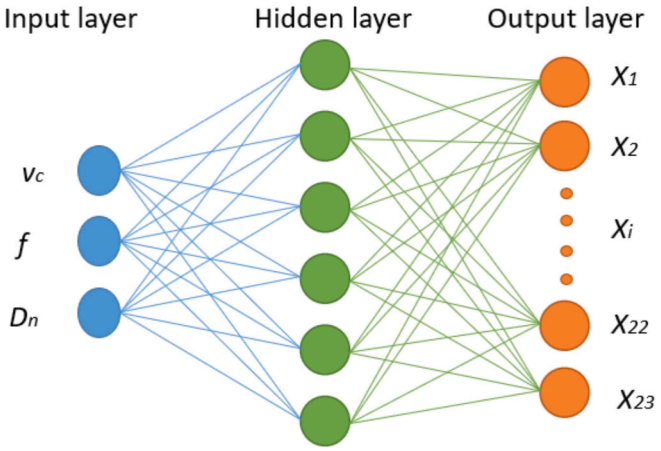

Fig. 2. ANN structure for predicting tool path as a function of v_c, f and D_n.

Table 4
Cutting parameters and final diameter.

v_c (m/min)	f (mm/rev)	a_p (mm)	D_n (mm)
60	0.10	1	18
			16
			14
			13
			11

cutting tool path (X_i) based on the nominal diameter, cutting speed, and feed rate (Fig. 2). The network, featuring a single hidden layer, was trained using the final trajectory (X_{3i}) obtained from the iterative turning process applied to specimens across various cutting parameters and diameter combinations.

The MATLAB R2022b software has been used to program the neural network. Hyperparameters for the network topology included the application of the sigmoid transfer function. Moreover, the Bayesian Regularisation backpropagation algorithm was selected because of its notably accurate performance. Training the ANN involved using 70% of the available data, while the remaining 30% was selected for validation. All computations were performed on an Intel(R) Core (TM) i7-12700F CPU (20 cores, 2.1 GHz) with 16 GB of RAM. The computational cost was low, with training times for each ANN model below 1 min.

To determine the number of neurons (N) in the hidden layer, the N value was chosen based on achieving the minimum Root Mean Square Error (RMSE). In addition, to validate the ANN, trajectories for 5 new specimens were generated, each with different values of cutting speed (v_c), feed rate (f), and nominal diameter (D_n) (Table 4). These parameters were selected to represent intermediate and previously untested machining conditions, ensuring a robust evaluation of the model's predictive capability. Using the predictions provided by the ANN, the specimens have been machined and measured using a millesimal micrometre.

To enhance the clarity of the experimental procedure, a flowchart (Fig. 3) has been included summarizing the full methodology followed in this study. The diagram outlines the definition of input parameters, the sequence of machining and measurement stages with iterative tool path compensations, and the development and validation of the ANN. It also highlights the relationship between the process variables and the resulting outputs, providing a comprehensive overview of the workflow and facilitating a better understanding of the applied approach.

3. Results

Fig. 4 shows the dimensional deviations throughout the machining operation for a set of specimens, varying the diameters from 18 mm (Fig. 4a) to 10 mm (Fig. 4e). The validation of this work was carried out through five new tests using different values of cutting speeds (40 and 80 m/min) and feed rates (0.05 and 0.15 mm/rev). In all the experimental conditions, the largest deviations from the nominal diameter were obtained in the section closest to the tailstock (Z = 225 mm), reaching an approximate deviation of 0.40 mm for the lowest v_c and f values (40 m/min and 0.05 mm/rev). Nevertheless, this deviation gradually decreased as machining progressed, coinciding with the approach of the cutting tool to the chuck.

Upon the first contact of the cutting tool with the material, workpiece deformation ensued, resulting in an increase in the final machined part diameter. Furthermore, in cases involving machine tools featuring a degree of clearance in mechanical components such as the tool slide, the tool response to material deformation tends to counteract this deformation, thereby contributing to an increase in the final diameter of the machined part, exceeding the specifications set in the numerical control programming.

In contrast, at the end of the chuck, where bending deformation was constrained, the workpiece exhibited rectified deflection as the cutting tool concluded the machining operation. In fact, the maximum

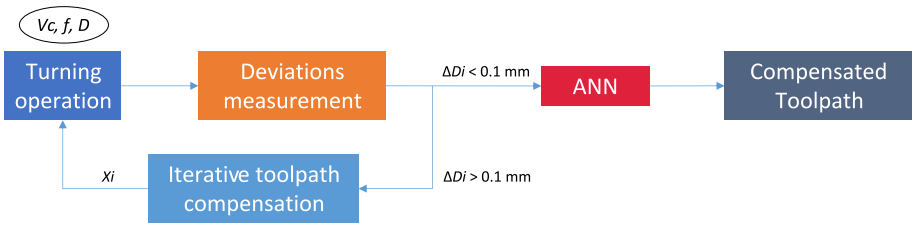

Fig. 3. Flowchart of the experimental procedure.

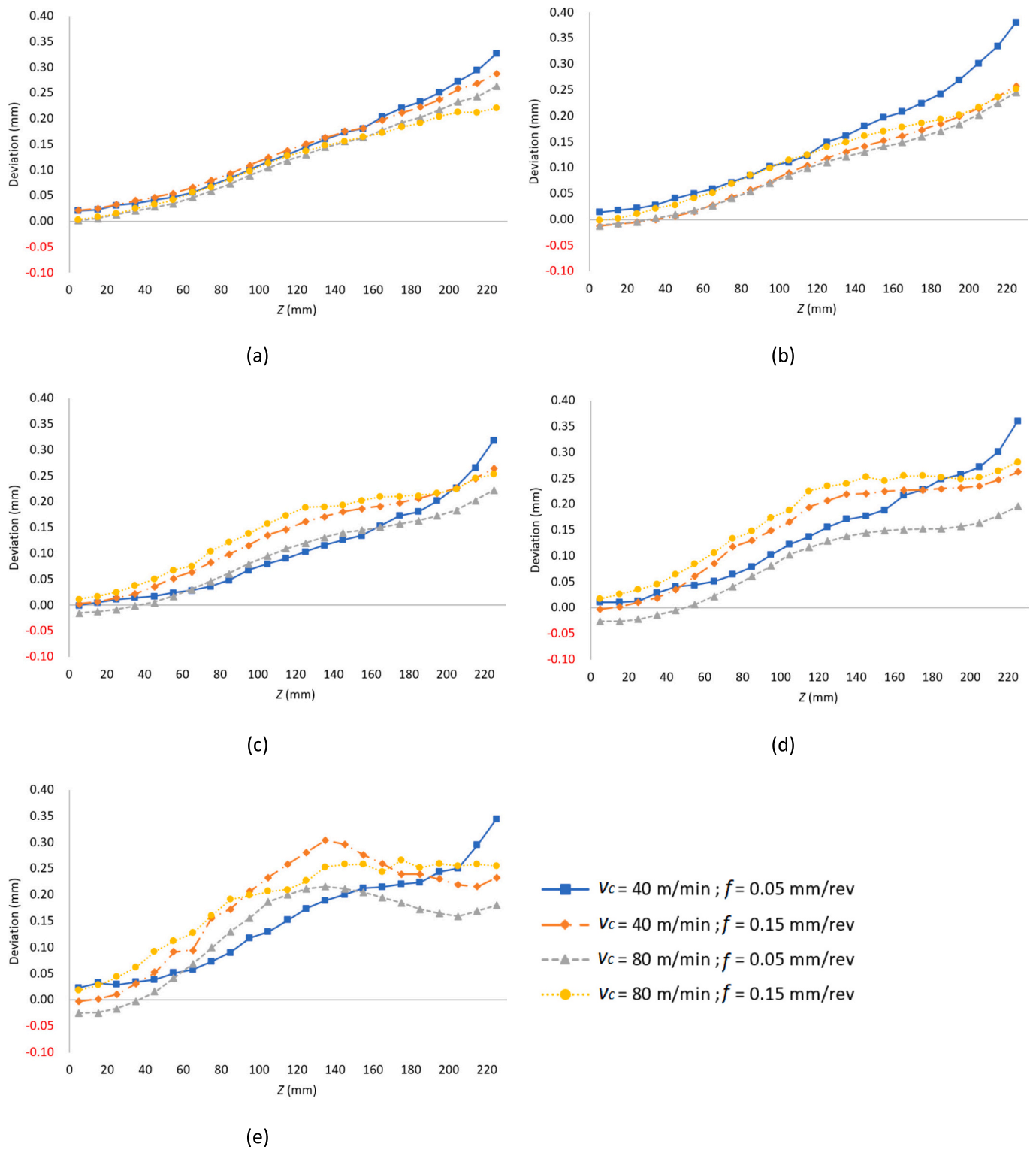

Fig. 4. Geometrical deviations for the samples turned with different v_c (40–80 m/min), f (0.05–0.15 mm/rev) and D_n (a) $D_n = 18$ mm, (b) $D_n = 16$ mm, (c) $D_n = 14$ mm, (d) $D_n = 12$ mm, (e) $D_n = 10$ mm.

deflection proximal to the chuck was consistently within 0.025 mm of the expected value in all cases.

The evolution of the deviation throughout the machining process exhibits a variability depending on the position relative to the chuck and tailstock. Initially, a notable decrease was observed, mainly due to the stabilisation resulting from tool contact and the simultaneous reduction in workpiece deformation as it moved away from the tailstock. This trend was particularly noticeable in the thicker samples (D_n 18 and 16 mm). Nevertheless, with the specimen diameter reduction, this change in behaviour highlighted the slenderness influence.

For the $D_n = 14$ mm specimen, the trend of decreasing deflection between Z = 120 and 200 mm was stabilised, remaining relatively constant within this range. Beyond Z = 120 mm, a notable deviation reduction ensued with continued machining, particularly in regions

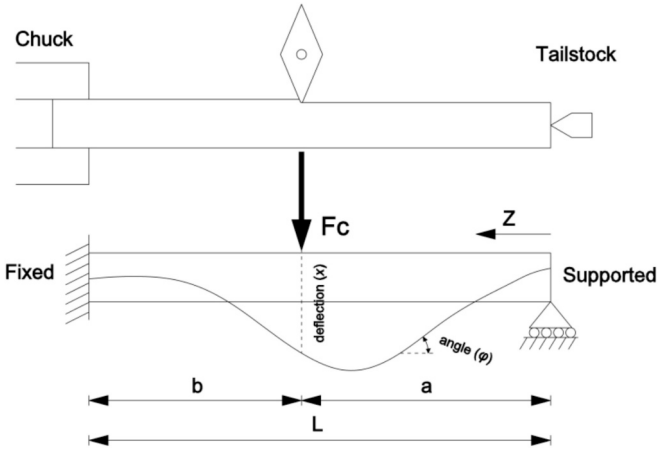

Fig. 5. Simplified mechanical model of the workpiece deflection during turning.

proximal to the chuck, where the deflection became negligible. A similar trend was observed for the $D_n = 12$ mm specimen, albeit with a slightly smaller initial reduction in deflection compared with the $D_n = 14$ mm specimen.

Within the slenderest specimen ($D_n = 10$ mm), this behaviour became increasingly evident over the range of positions. It is interesting to note that as the machining operation progressed, certain positions showed an escalation of the deflection.

This phenomenon can be explained by considering the turning operation of a part as similar to the behaviour of a beam subject to supported-fixed conditions under a point load moving in the machining direction. Strong clamping of the workpiece in the chuck can be likened to a fixed condition, while the tailstock represents a support, allowing greater freedom to deform in the Z direction (Fig. 5).

The cutting process involves the generation of a cutting force (Fc) perpendicular to the specimen generatrix. This force results in a deflection (x) and a deformation angle (φ) with respect to the horizontal. These values can be obtained from Eqs. (7) and (8), given the similarity of the turning process to a supported-fixed beam.

$$x = \frac{F_c b^2 Z}{12EIL^3}\left[3aL^2 - Z^2(2L+a)\right] \tag{7}$$

$$\varphi = -\frac{F_c a}{4EIL}(L-a)^2 \tag{8}$$

where a, b, and L are geometric characteristics, E is the elasticity modulus, and I correspond to the moment of inertia of a circular section beam.

The values of F_c depend on f, and E is a value corresponding to the material characteristics. The effect of slenderness on x and φ depend on

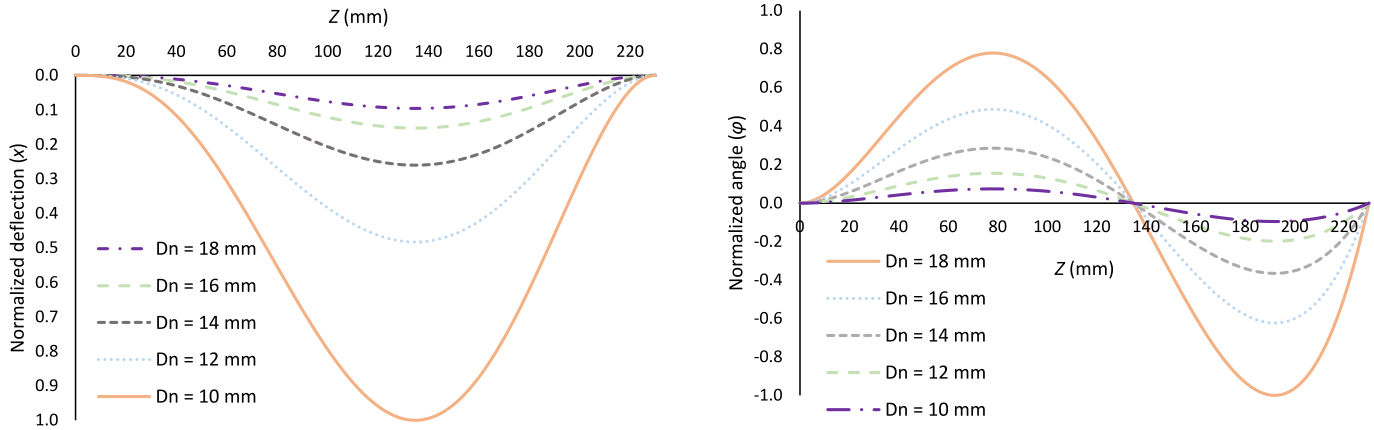

Fig. 6. Normalised deflection (x) and relative angle between the tool and the sample during machining.

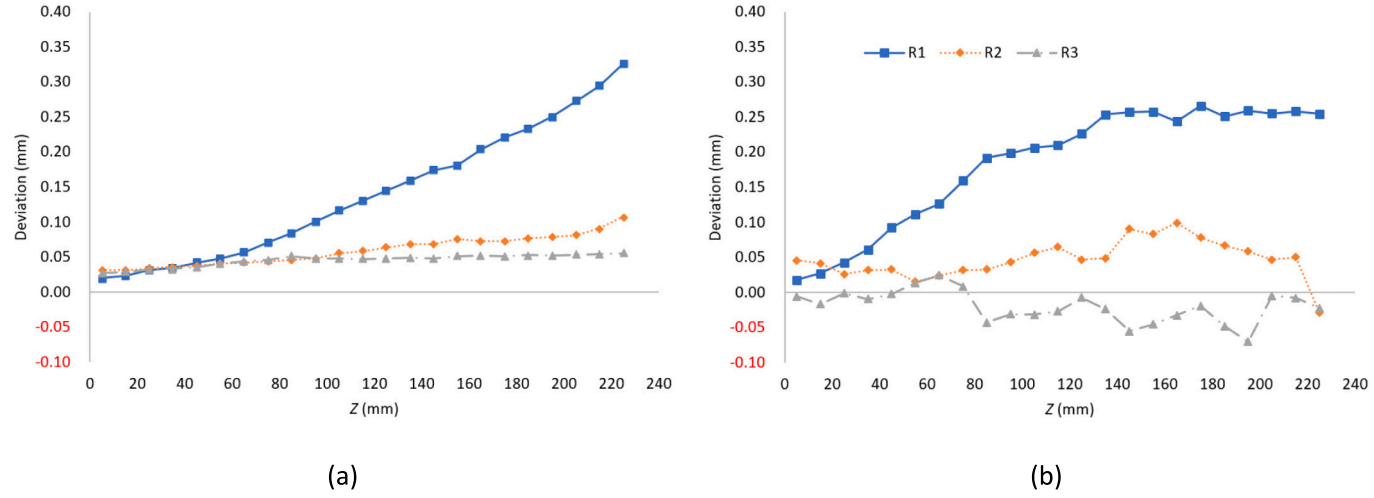

Fig. 7. Deviation evolution for different tool path compensations: (a) $v_c = 40$ m/min, $f = 0.05$ mm/rev, $D_n = 18$ mm; (b) $v_c = 80$ m/min, $f = 0.15$ mm/rev, $D_n = 10$ mm.

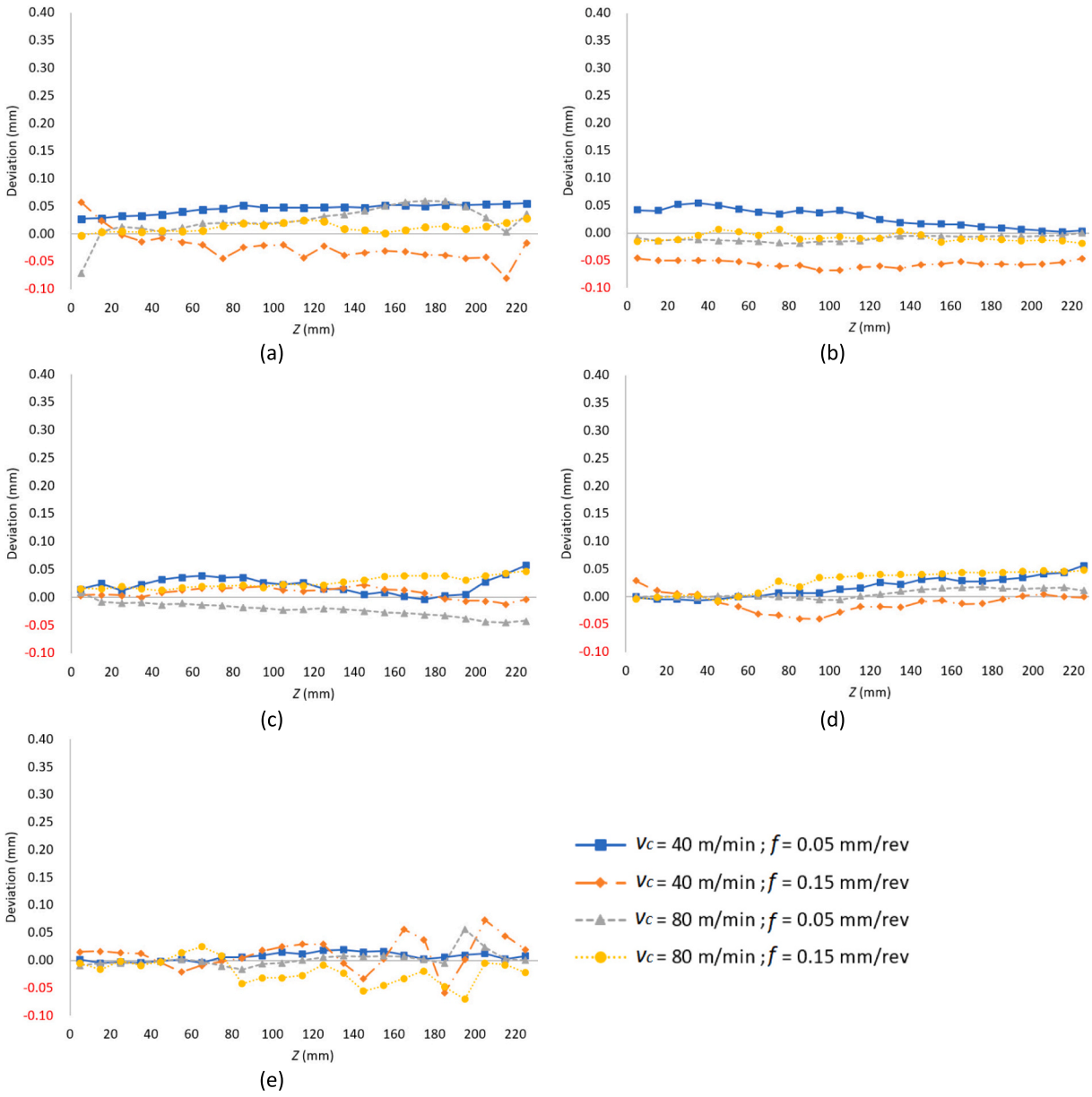

Fig. 8. Geometrical deviations for the samples turned after the third compensation (R3) with different v_c (40–80 m/min), f (0.05–0.15 mm/rev) and D_n (a) $D_n = 18$ mm, (b) $D_n = 16$ mm, (c) $D_n = 14$ mm, (d) $D_n = 12$ mm, (e) $D_n = 10$ mm.

D_n. Their values increase as D_n decreases. In Eqs. (7) and (8), this effect is determined from the inertia moment (Eq. (9)).

$$I = -\frac{\pi D_n^4}{32} \tag{9}$$

In an initial approach, the problem has been considered under static conditions, where F_c is assumed to remain constant throughout the turning process and E is treated as a fixed material property. Based on these assumptions, the deformation behaviour of the workpiece can be analysed in a simplified and normalised manner. Specifically, the deflection at each tool position along the Z-axis can be normalised in relation to the maximum deflection observed during machining. This allows the geometric influence to be evaluated independently of the absolute values of F_c or E. Similarly, the φ value can be addressed.

Fig. 6 shows the calculated normalised deflection (x) by the specimen at the tool position during machining, where L = 230 mm and a, b and Z values depend on the tool position. The results indicate that the maximum deflection occurs when the cutting tool is at Z = 135 mm. Around this position, the most significant deformations are observed, coinciding with the change in the trend towards reducing deviation from the nominal value discussed in the previous figure.

Regarding the deformation angle (φ) of the profile at the load point, the minimum value is obtained at Z = 192 mm, decreasing from the beginning of the machining operation until reaching this point. Within this range (190–230 mm), a rapid reduction in error compared to the nominal value is observed, with a noticeable softening once the tool surpasses Z = 190 mm. The rapid reduction in error compared with a positive angle is attributed to the increased tool freedom of movement.

Although the model has been considered static, it offers a practical approximation for identifying the regions most affected by deformation along the workpiece. The aim is not to capture the full dynamic behaviour of the process, but rather to isolate the geometric contribution, particularly the effect of slenderness, on the spatial distribution of deviations. Despite the simplifications, the results obtained are consistent with the experimental trends and support the validity of this approach.

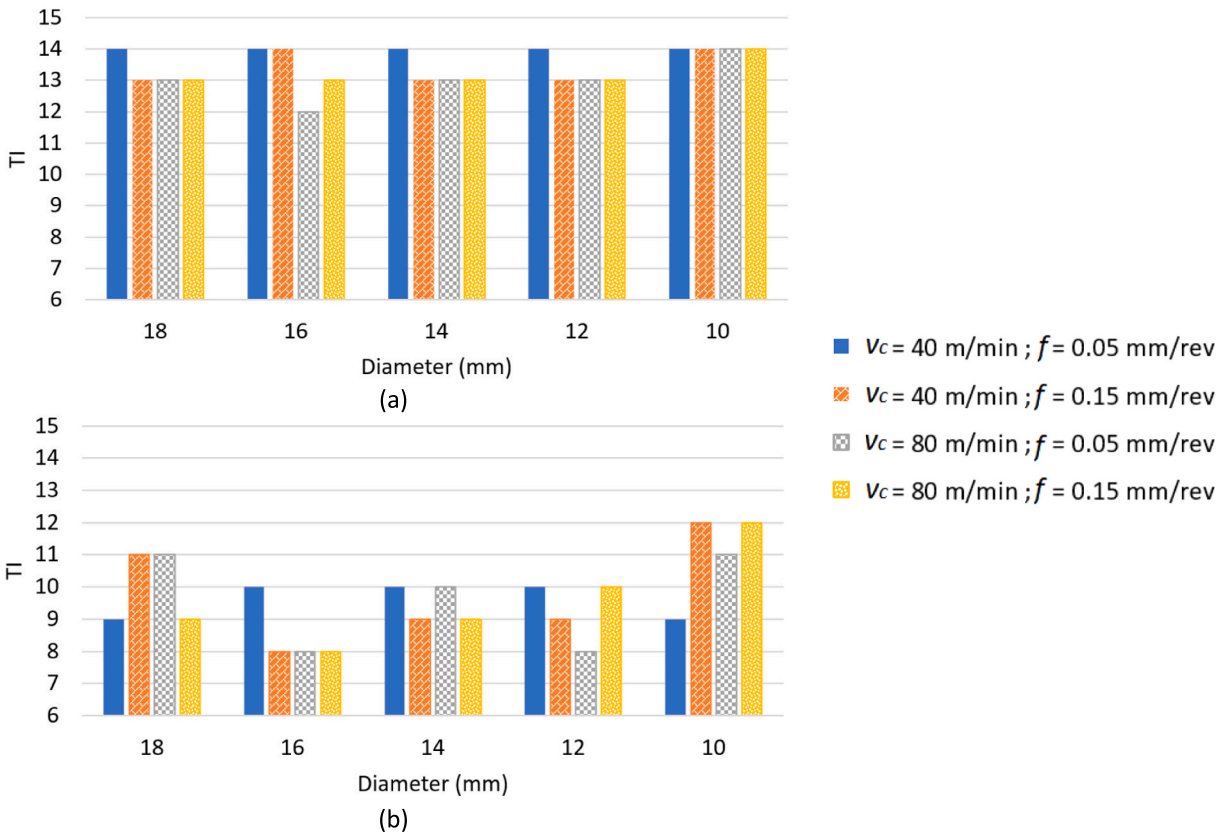

Fig. 9. Tolerance index in the turned specimens with different v_c (40–80 m/min), f (0.05–0.15 mm/rev): (a) without tool path compensation (R1) and (b) after the second tool path compensation (R3).

On the other hand, it is also important to note that in the region close to the chuck, for larger diameters (18 to 14 mm), the error obtained is minimal and nearly identical in all studied cases. For smaller D_n values, a higher deviation is observed, indicating that cutting parameters are a crucial aspect in the areas near the lathe chuck.

Regarding the influence of cutting parameters, it is noticeable that as the specimen diameter decreases (slender specimens), the cutting parameters exhibit a more significant influence. The influence of cutting speed (v_c) on dimensional deviation is not uniform, as it depends on the interaction with feed rate (f) and the slenderness of the part. At low f, increasing the v_c slightly reduces deviation because the cutting forces decrease and the tool–workpiece contact time shortens, producing a more stable process. However, at higher f, higher v_c increase vibration amplitude and cutting temperature, which amplifies elastic deformation and geometric error. This behaviour shows that the effect of v_c is governed by the balance between thermal expansion and dynamic instability, rather than by a single dominant mechanism.

For low feed rates (0.05 mm/rev), it is observed that specimens machined at a lower cutting speed (40 m/min) generally show a higher deviation compared to those machined at higher v_c values (80 m/min). Only the slenderest specimen ($D_n = 10$ mm) had higher deviations, being observed in the central area at high v_c. This could be attributed to tool vibration and higher deformation during turning in this central zone. A higher v_c is associated with a vibration increment, both of which contribute to the increase in the geometry error of the final part. However, for high f values (0.15 mm/rev), worse results were obtained for high v_c values. This could be related to a combination of thermal effects and increased vibrations, where high f values tend to increase the effect of both factors on geometric errors, with vibrations playing a more important role. It is noteworthy that the variation in v_c (40–80 m/min) is not significant enough for thermal effects to outweigh the impact of vibrations generated during machining.

Furthermore, the influence of f can be explained in terms of the cutting forces. Regardless of the v_c value, it can be observed that higher f values (0.15 mm/rev) exhibit greater deviations from the nominal value than lower f values (0.05 mm/rev). This is because an increase in f is associated with higher cutting forces, which tend to augment the workpiece deformation during machining, negatively affecting the deviation from the nominal value.

Similar trends have been reported in studies involving AISI 1045 steel [49,50] which identified the workpiece slenderness and feed as key factors influencing dimensional deviations. These results confirm that increased slenderness leads to greater deflection and geometric inaccuracies, which is consistent with the trends observed in this study for aluminium alloy UNS A97075-T6. Additionally, in dry turning of hardened steel research [51], the role of cutting forces and vibrations in dimensional error generation has been highlighted, especially at higher cutting speeds and feed values. This supports the present findings, where slender specimens exhibited greater deviations due to increased dynamic instability during machining.

After turning and measuring each sample (R1), the numerical control code was modified to compensate the trajectory of the cutting tool. Once the second sample (R2) has been obtained, the measurement and tool path adjustment was repeated and applied to obtain the third sample (R3). Fig. 7 shows the evolution of the deviations obtained in each compensation for the most extreme combinations of v_c, f, and D_n.

It can be seen that the part obtained after the first compensation (R2) significantly reduces the deflections of the specimen, the correction being greater in the area of the specimen closest to the tailstock, where there were initially greater deflections. Furthermore, in both cases, samples with deviations less than 0.1 mm were obtained, which was the initial objective. An average reduction of 39% over the whole part and a reduction of 67% at the point of maximum deviation is obtained. With the third adjustment of the trajectory (R3), the final geometry of the part

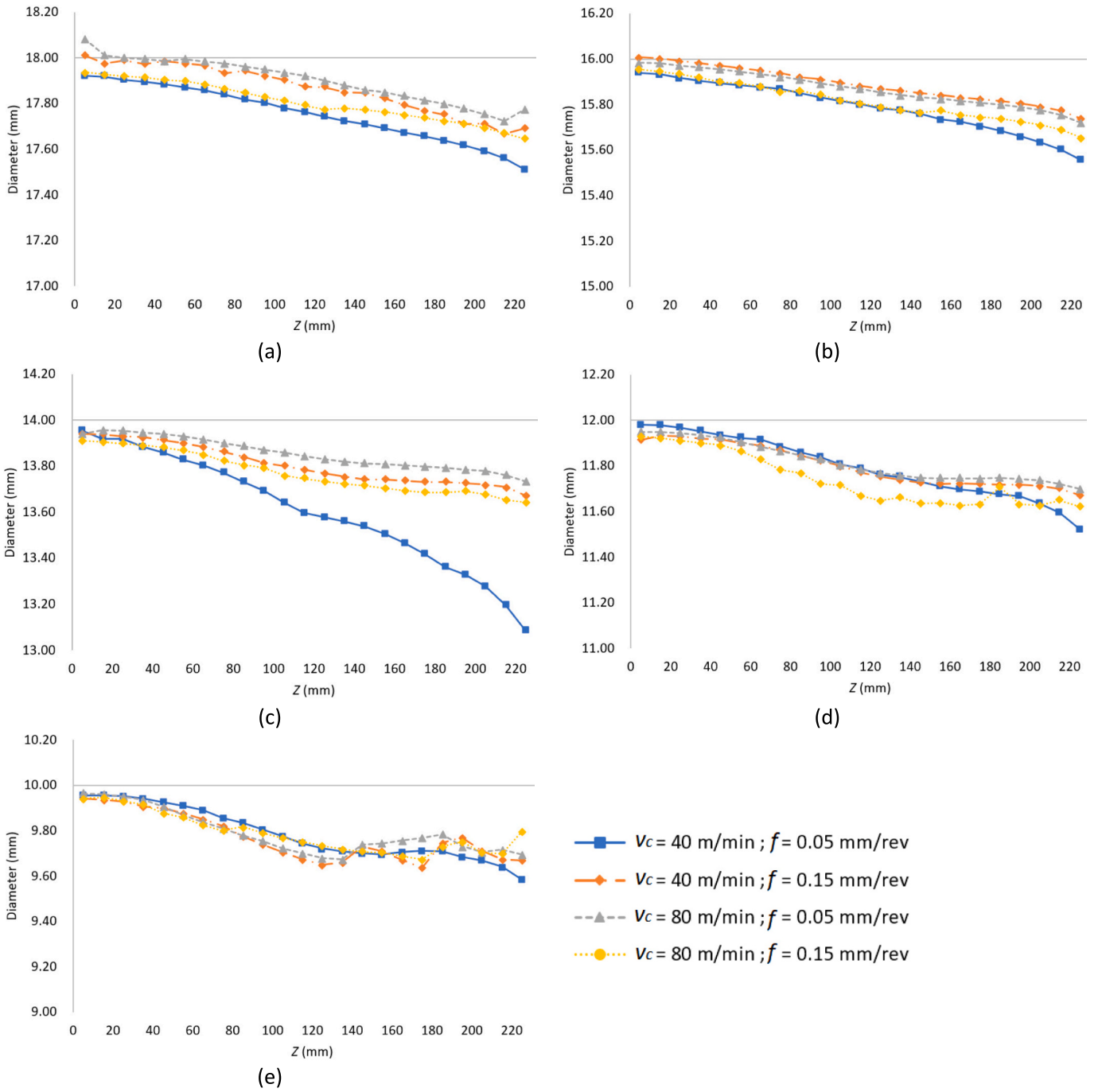

Fig. 10. Final tool path compensation for the different specimens machined with v_c (40–80 m/min), f (0.05–0.15 mm/rev) and D_n (a) $D_n = 18$ mm, (b) $D_n = 16$ mm, (c) $D_n = 14$ mm, (d) $D_n = 12$ mm, and (e) $D_n = 10$ mm.

was further improved, achieving a reduction of up to 87% of the deviations average obtained at the measured points in some cases, corresponding to those with greater slenderness ($D_n = 10$ mm).

In the case of softer machining conditions ($v_c = 40$ m/min, $f = 0.05$ mm/rev, $D_n = 18$ mm), with the first compensation (R2), the deviations have already been significantly reduced, but there is still a slight difference between the measurements taken at the points close to the chuck and those close to the lathe tailstock. With the second compensation (R3), a sample with a diameter value that was practically constant over its entire length was obtained. Conversely, under the most severe machining conditions ($v_c = 80$ m/min, $f = 0.15$ mm/rev, $D_n = 10$ mm), the first compensation (R2) produces a part with much smaller deviations, but these values are irregular along the length of the part. Although the error obtained in the final geometry of the machined part is smaller than the previous one, the same thing happens after the second compensation. This irregular behaviour is mainly due to the increase in vibrations caused by machining and the increase in cutting force, which causes greater deformation of the specimen.

After the third tool path compensation, all specimens showed a deviation of less than 0.10 mm from the nominal value, which was in line with the maximum deviation initially set (Fig. 8). Under these conditions, the deviation tends to stabilise throughout the turning process. However, components machined with high values of f (0.15 mm/rev) exhibit increased deflection variation along the machining length. This variation is attributed to increased vibration at higher f values, which cause minor fluctuations in part deflection.

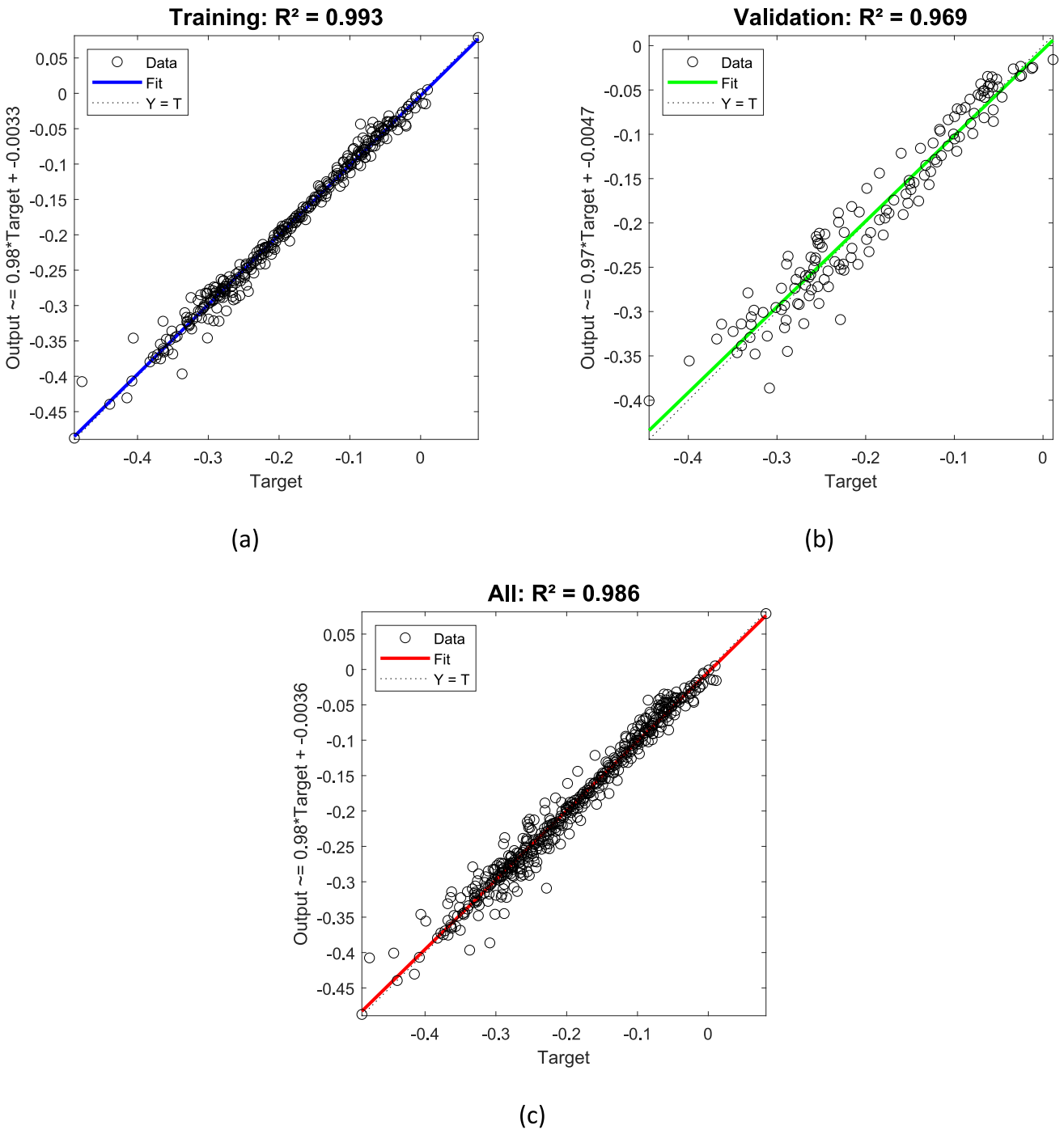

Fig. 11. ANN regression results for training, validation, and complete datasets.

It is important to note that for larger D_n values (18–16 mm), the compensation had a negative impact on the deflection in the region proximal to the chuck, slightly increasing its value. Nevertheless, the initial variability observed for smaller D_n values (14–10 mm) decreased, resulting in consistently low deviation regardless of the cutting parameters used.

In the design and component manufacture, the industry commonly uses standardised tolerance values. These values are defined in the ISO 286–2 standard [52], which establishes tolerance indexes (TI) based on the nominal diameter of the part. Fig. 9a shows the TIs of each machined sample, considering the maximum deviation obtained in the machining of the specimens without compensating the tool path. The results indicate that the highest TI value is achieved at low v_c values (40 m/min) and low f values (0.05 mm/rev), resulting in higher tolerance values than the nominal value. However, all cases studied resulted in an IT14 in a D_n of 10 mm. This is because although no significant deviations from the nominal value were observed, the normalised tolerance decreased for diameters smaller than 10 mm.

After path compensation, the TIs of the evaluated samples (Fig. 9b) are lower than those of the uncompensated samples due to the reduction of deviations. The reduction in TI values is more noticeable for larger diameters (12–18 mm) than for the slenderest part (10 mm), although an improvement is always obtained in all cases.

After the sample had been machined with the second tool path compensation (R3), the final compensation was determined based on the diameter measurements obtained at different points of the sample. This

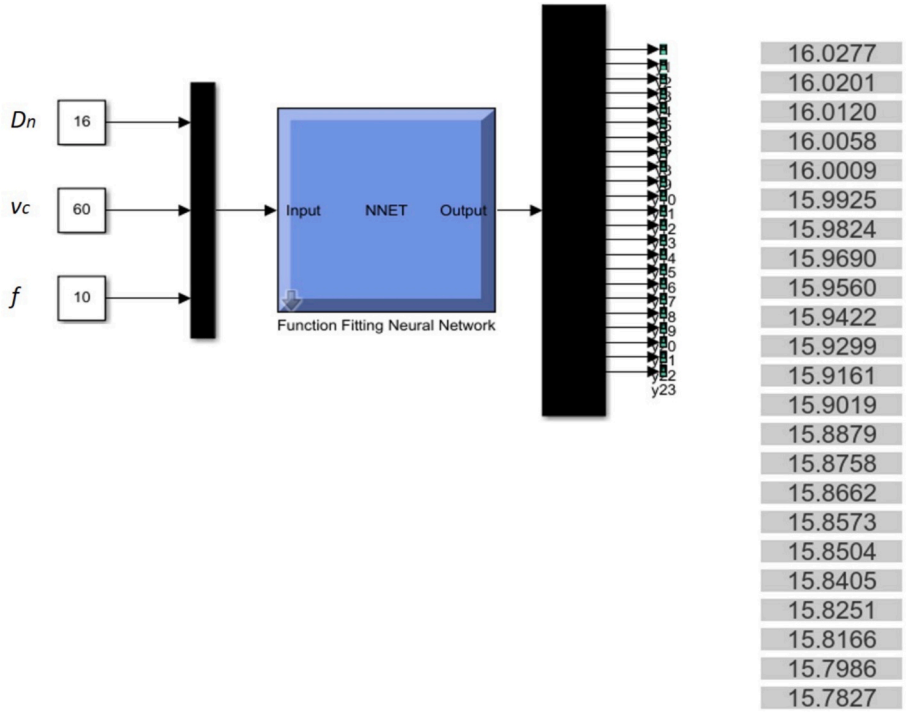

Fig. 12. Tool path prediction with Simulink for $v_c = 60$ m/min, $f = 0.10$ mm/rev, and $D_n = 16$ mm.

was used to adjust the final geometry of the specimen with respect to its nominal value. The results of the trajectories with this final compensation for each case studied are shown in Fig. 10.

The final trajectories exhibit a similar behaviour to the results obtained during the first machining of the specimens, except that the deviations presented by the trajectories are below the nominal diameter value.

For high D_n values (18–16 mm), the trajectory approaches the nominal value as machining progresses. The variation is more pronounced at the beginning of machining near the tailstock. In case of smaller D_n (14–10 mm), the trajectory tends not to show any variation in the zones of maximum deformation (Z = 200–120 mm). Therefore, these results are aligned with the main objective of reducing deviations in the machined parts.

A Feedforward neural network has been developed using the final trajectories of cutting tools to predict trajectories under different conditions than those used during the experimental process. This allows the production of parts with a diameter deviation from the nominal value of less than 0.10 mm without the need for an iterative process of machining and measuring the specimen.

Various neural network topologies were evaluated using 70% of the dataset for training and 30% for validation. Within the studied parameter space, an ANN with a single hidden layer of 5 neurons provided the best trade-off between prediction accuracy, model stability and computational efficiency, yielding an RMSE of 0.0006 mm in training and 0.0012 mm in validation, with an overall fit of $R^2 = 0.98$ (Fig. 11). These indicators quantify the statistical accuracy of the ANN for predicting the compensated trajectory, where R^2 reflects the correlation between predicted and experimental tool-path points and RMSE represents the average magnitude of the prediction error. Importantly, the objective of the proposed model is not ultra-high-precision machining at the micrometre level, but to predict a compensated tool path that enables final diameter deviations to remain within ±0.10 mm for slender parts under dry turning conditions. In this context, the achieved accuracy demonstrates that a lightweight architecture is sufficient and practical, allowing the ANN to be reliably used to predict the tool path for new cutting conditions.

The iterative corrections were performed only during the experimental phase to generate the training dataset. Once trained, the ANN predicts the compensated tool path directly, without requiring further iteration.

The application of ANN enables the prediction of cutting tool trajectory for new parts with different conditions from those used in the experimental part for network training and validation. The validation of this work was carried out through five new tests using different values of v_c, f, and D_n from those previously performed (Table 4). The path points were obtained using the Simulink module in Matlab (Fig. 12).

Fig. 13 shows the predicted tool path and the measured dimensions of the machined parts after implementing the obtained trajectory. In all cases, the first machining operation produced a part that met the proposed objective of a deviation of less than 0.10 mm from the nominal value, without the need for an iterative process to determine the necessary compensation. The proposed methodology is considered valid because it reduces material costs and working time while ensuring dimensional tolerances in the machined parts.

It is important to note that in certain cases, such as $D_n = 18$ mm and $D_n = 13$ mm, the deviations are greater than those obtained through the iterative process. However, in the remaining three cases, the variation is significantly smaller and can be considered practically constant. In fact, in the most unfavourable scenario, where $D_n = 11$ mm, this variation is even lower than that obtained by the iterative process for the smaller diameter parts ($D_n = 10$ mm). Thus, it can be considered that the effect of vibrations during machining is considered by the ANN when predicting the trajectory. However, it is worth noting that deviations near the chuck are greater in specimens compensated by ANN than in those compensated by iteration. Despite this, the specimens compensated by the ANN can still be considered valid according to the proposed objective.

Regarding the trajectory prediction, it is important to note that for the slenderest parts ($D_n = 14$–11 mm), the deformation of the specimen caused by cutting forces has been considered. This results in a smoother variation in X of the trajectory in machining progresses within the range of Z values between 120 and 200 mm.

Recent advances have demonstrated the potential of ANN to improve

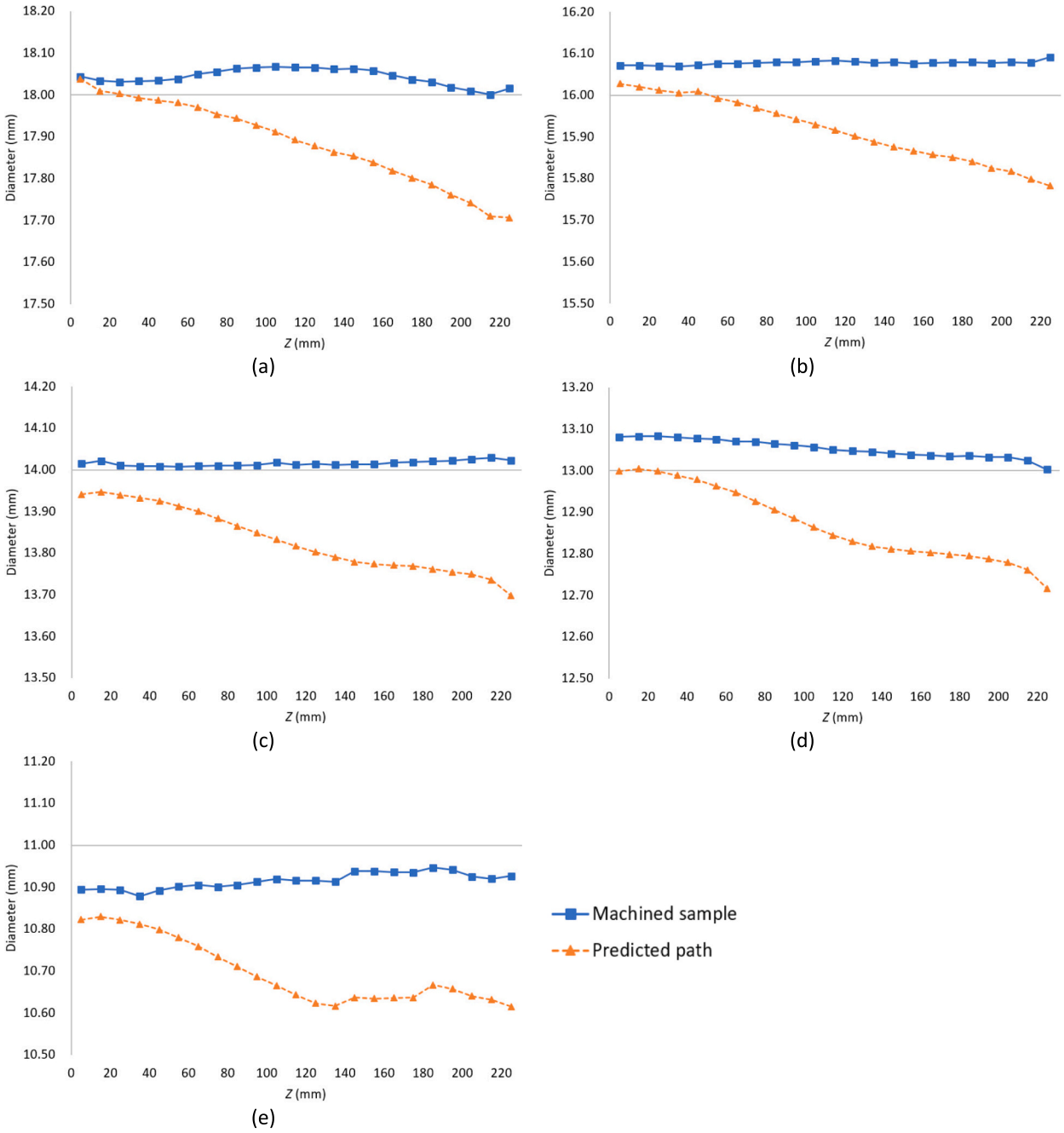

Fig. 13. Predicted path and machined samples of ANN validation tests for vc = 60 m/min and f = 0.10 mm/rev: (a) $D_n = 18$ mm, (b) $D_n = 16$ mm, (c) $D_n = 14$ mm, (d) $D_n = 13$ mm, and (e) $D_n = 11$ mm.

tool path accuracy in machining. Zhang et al. [53] proposed a back-propagation neural network for predicting step errors in tool paths during the machining of freeform surfaces. Their model achieved predictions deviating less than 1 μm from theoretical values, and demonstrated significant computational efficiency compared to conventional geometric approaches. However, their work focused primarily on geometric interpolation errors in surface generation.

In contrast, the present study employs an ANN to predict and compensate dimensional deviations arising from mechanical effects, such as deflection, vibration, and tool–workpiece interaction. This approach addresses a different class of error, driven by part flexibility and cutting dynamics, rather than surface geometry alone. While both methods aim to enhance machining precision through data-driven prediction, the current model is specifically tailored to deformation-induced errors in turning operations involving slender geometries.

Finally, to validate the ANN, the TI of each of the machined parts was determined. As it can be seen in Fig. 14, lower TI values were obtained for the parts machined with trajectory compensation, going from a TI of 13 to a TI of 11 in the worst of the cases evaluated. It should be noted that in two of the cases, the TI value is 8, which can be considered as high-quality parts in terms of geometric control.

4. Conclusions

This study investigated the dimensional deviations occurring in dry turning operations of UNS A97075-T6 aluminium alloy, focusing particularly on the influence of part slenderness and the optimisation of tool path strategies. A novel methodology was proposed to compensate

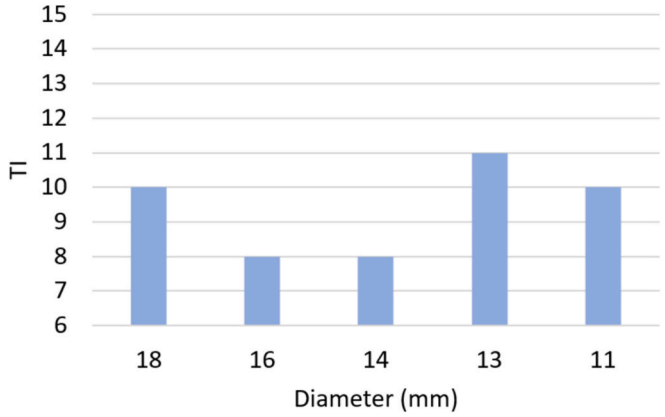

Fig. 14. ANN validation samples TI for different diameters.

for these deviations through both an iterative correction process and an Artificial Neural Network based prediction system.

The experimental results revealed that dimensional deviations followed a nonlinear trend, strongly influenced by the relative position along the workpiece and its slenderness. Maximum deviations of up to 0.40 mm were observed in the most flexible specimens (nominal diameter of 10 mm), particularly in the region close to the tailstock. These deviations were progressively reduced by implementing a three-step iterative tool path compensation, achieving final errors below 0.10 mm, with an average error reduction of 87% and a maximum reduction of 67% at the most critical locations.

In parallel, a feedforward ANN was trained using cutting speed, feed and nominal diameter as input parameters. The model achieved $R^2 = 0.98$ and RMSE = 0.0012 mm in testing, allowing for accurate first-pass tool path prediction. Validation experiments demonstrated that ANN-predicted paths resulted in dimensional deviations within the targeted tolerance range (±0.10 mm), without requiring iterative compensation. Tolerance Index values improved from IT13–14 to IT8–11, depending on the specimen diameter, which corresponds to a significantly higher level of dimensional quality.

Compared to previous approaches, this work offers a direct and effective method to compensate geometrical deviations in slender parts. Importantly, the ANN can capture the combined effects of deflection, vibrations and tool–workpiece interactions without measuring them explicitly, simplifying its practical implementation.

From an industrial perspective, the proposed method reduces the need for repeated machining and inspection cycles, decreases total production time and cost, and avoids the use of cutting fluids, supporting sustainable manufacturing practices. The approach is particularly beneficial in aerospace and automotive components, where thin-walled aluminium parts are increasingly used and dimensional tolerances are critical.

The proposed method operates offline, avoiding the need for additional sensors or integration with the CNC controller. This simplifies implementation and significantly reduces equipment and maintenance costs while maintaining process repeatability under similar machining conditions. Although real-time compensation systems can provide higher adaptability, they require costly instrumentation and complex integration. Future work will focus on developing hybrid approaches that combine predictive and sensor-based compensation to improve flexibility and adaptability in industrial environments.

It is important to notice that tool wear was not considered in the present predictive model, since a new cutting edge was used in each test to isolate the effects of cutting parameters and part slenderness. As wear can influence dimensional accuracy over extended production cycles, future work will incorporate wear information, such as machining time or other suitable indicators, as additional inputs to improve model robustness and industrial applicability.

Finally, it should be noted that the developed ANN is valid within the range of cutting parameters studied. For operating conditions outside this range, new experimental data would be required to retrain the network using the same methodology to ensure predictive accuracy. Therefore, this research not only confirms the critical role of slenderness in machining accuracy but also provides a practical and generalisable solution to predict and correct tool paths for improved dimensional control in CNC turning of lightweight alloys.

CRediT authorship contribution statement

S. Martín-Béjar: Conceptualization, Methodology, Software, Formal analysis, Data curation, Investigation, Writing - original draft, Writing - review and editing. **F.J. Trujillo:** Conceptualization, Software, Formal analysis, Resources, Writing - review and editing. **F. Bañón:** Methodology, Investigation, Visualization, Writing - review and editing. **C. Bermudo:** Data Curation, Investigation, Visualization, Writing - review and editing. **L. Sevilla:** Conceptualization, Supervision, Writing, review and editing, Funding adquisition.

Funding

Funding for open access charge: Universidad de Málaga / CBUA. This work has received funding from the Spanish Office of Science and Innovation, through the research project “Expert system for improving surface integrity in sustainable machining of light alloys (SPAREMETAL)”, with reference PID2021-125988OB-I00.

Declaration of competing interest

The authors declare that they have no known competing financial interests or personal relationships that could have appeared to influence the work reported in this paper.

Acknowledgments

The authors thank the University of Malaga-Andalucia Tech Campus for its contribution to this work.

Data availability

The data that support the findings of this study are available from the corresponding author upon reasonable request.

References

[1] Dantan JY, Mathieu L, Ballu A, Martin P. Tolerance synthesis: quantifier notion and virtual boundary. Comput Aided Des 2005;37(2):231–40. https://doi.org/10.1016/j.cad.2004.06.008.
[2] Bouvet C. Mechanics of aeronautical composite materials. In: Mechanics of aeronautical composite materials; Aug. 2017. https://doi.org/10.1002/9781119459057.
[3] Irani SA, Mittal RO, Lehtihet EA. Tolerance chart optimization. Int J Prod Res 1989;27(9):1531–52. https://doi.org/10.1080/00207548908942638.
[4] Sweet AL, Tu JF. Evaluating tolerances and process capability when using truncated probability density functions. Int J Prod Res Sep. 2006;44(17):3493–508. https://doi.org/10.1080/00207540500521576.
[5] Geng Z, Bidanda B. Tolerance estimation and metrology for reverse engineering based remanufacturing systems. Int J Prod Res May 2022;60(9):2802–15. https://doi.org/10.1080/00207543.2021.1904158.
[6] Minetola P, Galati M, Calignano F, Iuliano L, Rizza G, Fontana L. Comparison of dimensional tolerance grades for metal AM processes. Procedia CIRP Jan. 2020;88:399–404. https://doi.org/10.1016/J.PROCIR.2020.05.069.
[7] Rupal BS, Anwer N, Secanell M, Qureshi AJ. Geometric tolerance and manufacturing assemblability estimation of metal additive manufacturing (AM) processes. Mater Des Sep. 2020;194:108842. https://doi.org/10.1016/J.MATDES.2020.108842.
[8] Ramesh R, Mannan MA, Poo AN. Error compensation in machine tools — a review: part I: geometric, cutting-force induced and fixture-dependent errors. Int J Mach Tool Manuf Jul. 2000;40(9):1235–56. https://doi.org/10.1016/S0890-6955(00)00009-2.

[9] De Agustina B, Rubio EM. Analysis of cutting forces during dry turning processes of UNS A92024-T3 aluminium bars. In: AIP conference proceedings; 2012. p. 360–5. https://doi.org/10.1063/1.4707584.

[10] De Agustina B, Rubio EM, Sebastián MÁ. Surface roughness predictive model of UNS A97075 aluminum pieces obtained by dry turning tests based on the cutting forces. Appl Mech Mater 2012:1628–35. https://doi.org/10.4028/www.scientific.net/AMM.217-219.1628.

[11] Ranjan Soren T, Kumar R, Panigrahi I, Kumar Sahoo A, Panda A, Kumar Das R. Machinability behavior of aluminium alloys: a brief study. Mater Today Proc 2019; 18:5069–75. https://doi.org/10.1016/j.matpr.2019.07.502.

[12] Santos MC, Machado AR, Sales WF, Barrozo MAS, Ezugwu EO. Machining of aluminum alloys: a review. Int J Adv Manuf Technol Oct. 2016;86(9–12):3067–80. https://doi.org/10.1007/s00170-016-8431-9.

[13] Pimenov DY, et al. Review of improvement of machinability and surface integrity in machining on aluminum alloys. Int J Adv Manuf Technol Dec. 2023;129(11–12): 4743–79. https://doi.org/10.1007/s00170-023-12630-4.

[14] Romero PE, Dorado R, Díaz Garrido FA, Rubio EM. Relationship of pocket geometry and tool path strategy with 2 1/2-D milling parameters: machining time, cutting forces and surface roughness. Mater Sci Forum Jun. 2014;797:78–83. https://doi.org/10.4028/www.scientific.net/MSF.797.78.

[15] Srivastava AK, Veldhuis SC, Elbestawit MA. Modelling geometric and thermal errors in a five-axis cnc machine tool. Int J Mach Tool Manuf 1995;35(9):1321–37. https://doi.org/10.1016/0890-6955(94)00048-O.

[16] Andolfatto L, Lavernhe S, Mayer JRR. Evaluation of servo, geometric and dynamic error sources on five-axis high-speed machine tool. Int J Mach Tool Manuf Oct. 2011;51(10–11):787–96. https://doi.org/10.1016/J.IJMACHTOOLS.2011.07.002.

[17] Vahebi M, Arezoo B. Accuracy improvement of volumetric error modeling in CNC machine tools. Int J Adv Manuf Technol Mar. 2018;95(5–8):2243–57. https://doi.org/10.1007/S00170-017-1294-X/METRICS.

[18] Okafor AC, Ertekin YM. Derivation of machine tool error models and error compensation procedure for three axes vertical machining center using rigid body kinematics. Int J Mach Tool Manuf Jun. 2000;40(8):1199–213. https://doi.org/10.1016/S0890-6955(99)00105-4.

[19] Bohez ELJ, Ariyajunya B, Sinlapeecheewa C, Shein TMM, Lap DT, Belforte G. Systematic geometric rigid body error identification of 5-axis milling machines. Comput Aided Des Apr. 2007;39(4):229–44. https://doi.org/10.1016/J.CAD.2006.11.006.

[20] Leach RK, Bourell D, Carmignato S, Donmez A, Senin N, Dewulf W. Geometrical metrology for metal additive manufacturing. CIRP Ann Jan. 2019;68(2):677–700. https://doi.org/10.1016/J.CIRP.2019.05.004.

[21] Tekkalmaz M, Er Ü, Çakir FH, Bozkurt F. A new approach to monitor wear tracks propagation on-site with electromechanical impedance technique. J Intell Mater Syst Struct Jan. 2022;33(2):342–51. https://doi.org/10.1177/1045389X211014951.

[22] Das D, Dash SK, Rauniyar RK, Suaeb Ahemad SMd, Kumar R, Samal C. Turning investigations of Al 7075 alloy with ZrCN-coated WC inserts: parametric optimization and cutting temperature prediction. In: Lecture notes in mechanical engineering. Springer Science and Business Media Deutschland GmbH; 2023. p. 531–42. https://doi.org/10.1007/978-981-19-4388-1_45.

[23] Müller B, Renz U, Hoppe S, Klocke F. Radiation thermometry at a high-speed turning process. American Society of Mechanical Engineers (ASME); 2004. https://doi.org/10.1115/1.1763188.

[24] Srivastava A, Verma MK, Niranjan RS, Chandra A, Patel PB. Experimental investigation and optimization of machining parameters in turning of aluminum alloy 075-T651. Prod Eng Arch Dec. 2021;27(4):296–305. https://doi.org/10.30657/pea.2021.27.40.

[25] Abas M, et al. Experimental investigation and statistical evaluation of optimized cutting process parameters and cutting conditions to minimize cutting forces and shape deviations in Al6026-T9. Materials Oct. 2020;13(19):1–21. https://doi.org/10.3390/ma13194327.

[26] Aouici H, Bouchelaghem H, Yallese MA, Elbah M, Fnides B. Machinability investigation in hard turning of AISI D3 cold work steel with ceramic tool using response surface methodology. Int J Adv Manuf Technol 2014;73(9–12):1775–88. https://doi.org/10.1007/s00170-014-5950-0.

[27] Mohan Reddy M, Kumar M, Shanmugam K. Finite element analysis and modeling of temperature distribution in turning of titanium alloys. Metall Mater Eng Apr. 2018;24(1):59–69. https://doi.org/10.30544/323.

[28] Lokesha, Nagaraj PB, Dinesh P. Experimental investigation of machine tool condition during machining of ferrous components. Int J Mech Eng Robot Res Jan. 2018;7(1):72–7. https://doi.org/10.18178/ijmerr.7.1.72-77.

[29] Yousefi S, Zohoor M. Effect of cutting parameters on the dimensional accuracy and surface finish in the hard turning of MDN250 steel with cubic boron nitride tool, for developing a knowledged base expert system. Int J Mech Mater Eng Dec. 2019; 14(1). https://doi.org/10.1186/s40712-018-0097-7.

[30] Şahinoğlu A, Karabulut Ş, Güllü A. Study on spindle vibration and surface finish in turning of Al 7075. Solid State Phenomena Aug. 2017;261:321–7. https://doi.org/10.4028/www.scientific.net/SSP.261.321.

[31] Martín-Béjar S, Trujillo Vilches FJ, Gamboa CB, Hurtado LS. Cutting speed and feed influence on surface microhardness of dry-turned UNS A97075-T6 alloy. Appl Sci (Switzerland) Feb. 2020;10(3). https://doi.org/10.3390/app10031049.

[32] Habibi M, Arezoo B, Vahebi Nojedeh M. Tool deflection and geometrical error compensation by tool path modification. Int J Mach Tool Manuf 2011;51(6): 439–49. https://doi.org/10.1016/j.ijmachtools.2011.02.005.

[33] Pahk HJ, Lee SW. Thermal error measurement and real time compensation system for the CNC machine tools incorporating the spindle thermal error and the feed axis thermal error. 2002.

[34] Zhang Z, Cai L, Cheng Q, Liu Z, Gu P. A geometric error budget method to improve machining accuracy reliability of multi-axis machine tools. J Intell Manuf Feb. 2019;30(2):495–519. https://doi.org/10.1007/s10845-016-1260-8.

[35] Downey J, O'Leary P, Raghavendra R. Comparison and analysis of audible sound energy emissions during single point machining of HSTS with PVD TiCN cutter insert across full tool life. Wear May 2014;313(1–2):53–62. https://doi.org/10.1016/j.wear.2014.02.004.

[36] Zhou JM, Andersson M, Stahl JE. The monitoring of flank wear on the CBN tool in the hard turning process. Int J Adv Manuf Technol 2003;22(9–10):697–702. https://doi.org/10.1007/s00170-003-1569-2.

[37] Wang SM, Chen YS, Lee CY, Yeh CC, Wang CC. Methods of in-process on-machine auto-inspection of dimensional error and auto-compensation of tool wear for precision turning. Appl Sci 2016;6(5). https://doi.org/10.3390/app6040107.

[38] Kannan TDB, kannan GR, Kumar BS, Baskar N. Application of artificial neural network modeling for machining parameters optimization in drilling operation. Procedia Mater Sci 2014;5:2242–9. https://doi.org/10.1016/j.mspro.2014.07.433.

[39] Rodrigues A, Silva FJG, Sousa VFC, Pinto AG, Ferreira LP, Pereira T. Using an artificial neural network approach to predict machining time. Metals (Basel) Oct. 2022;12(10). https://doi.org/10.3390/met12101709.

[40] Kosarac A, Mladjenovic C, Zeljkovic M, Tabakovic S, Knezev M. Neural-network-based approaches for optimization of machining parameters using small dataset. Materials Feb. 2022;15(3). https://doi.org/10.3390/ma15030700.

[41] Chen N. An evolutionary neural network approach to machining process planning: a proof of concept. In: Procedia manufacturing. Elsevier B.V.; 2021. p. 690–6. https://doi.org/10.1016/j.promfg.2021.06.083.

[42] Yeo C, Kim BC, Cheon S, Lee J, Mun D. Machining feature recognition based on deep neural networks to support tight integration with 3D CAD systems. Sci Rep Dec. 2021;11(1). https://doi.org/10.1038/s41598-021-01313-3.

[43] Ponce MB, Illana IDS, Fernandez-Vidal SR, Gomez JS. Experimental parametric model for adhesion wear measurements in the dry turning of an AA2024 alloy. Materials Basel Sep. 2018;11(9):1598. https://doi.org/10.3390/MA11091598.

[44] Blanco D, Rubio EM, Lorente-Pedreille RM, Sáenz-Nuño MA. Sustainable processes in aluminium, magnesium, and titanium alloys applied to the transport sector: a review. MDPI Jan. 01, 2022. https://doi.org/10.3390/met12010009.

[45] Martín-Béjar S, Trujillo Vilches FJ, Gamboa CB, Hurtado LS. Cutting speed and feed influence on surface microhardness of dry-turned UNS A97075-T6 alloy. Appl Sci (Switzerland) Feb. 2020;10(3). https://doi.org/10.3390/app10031049.

[46] Rajasekaran T, Palanikumar K, Vinayagam BK. Application of fuzzy logic for modeling surface roughness in turning CFRP composites using CBN tool. Prod Eng Apr. 2011;5(2):191–9. https://doi.org/10.1007/S11740-011-0297-Y/FIGURES/13.

[47] Sauer K, Hertel M, Fickert S, Witt M, Putz M. Cutting parameter study of CFRP machining by turning and turn-milling. In: Procedia CIRP. Elsevier B.V.; 2020. p. 457–61. https://doi.org/10.1016/j.procir.2020.05.079.

[48] Farooq MU, Cooper D. Multi-fidelity machine learning framework for life cycle assessment: a manufacturing case study on aluminum rolling. Procedia CIRP 2025; 135:181–6. https://doi.org/10.1016/j.procir.2024.12.014.

[49] Núñez López PJ, Simao J, Rubio Alvir EM, Rincón JL. Influence of the machining parameters on workpiece roundness error during turning operations. Mater Sci Forum Oct. 2006;526:127–32. https://doi.org/10.4028/www.scientific.net/MSF.526.127.

[50] Filho ARS, Abrão AM, Paiva AP, Ferreira JR. Multivariate optimization of the cutting parameters when turning slender components. Int J Manuf Mater Mech Eng Oct. 2012;2(4):12–31. https://doi.org/10.4018/ijmmme.2012100102.

[51] Yousefi S, Zohoor M. Effect of cutting parameters on the dimensional accuracy and surface finish in the hard turning of MDN250 steel with cubic boron nitride tool, for developing a knowledged base expert system. Int J Mech Mater Eng Dec. 2019; 14(1):1. https://doi.org/10.1186/s40712-018-0097-7.

[52] International Standard Organization. ISO 286-2 Geometrical product specifications (GPS)-ISO code system for tolerances on linear sizes. 2010.

[53] Zhang Z-Y, Liu W, Li P-F, Zhang J-P, Fan L-Y. A numerical control machining tool path step error prediction method based on BP neural network. Sci Rep Sep. 2023; 13(1):16347. https://doi.org/10.1038/s41598-023-43617-6.